Photophysics of Methyl-Substituted Uracils and Thymines and Their Water Complexes in the Gas Phase

Yonggang He, Chengyin Wu, and Wei Kong*

Department of Chemistry, Oregon State University, Corvallis, Oregon 97331-4003

Received: August 27, 2003; In Final Form: December 2, 2003

We report studies on several methylated uracils and thymines and thymine−water complexes in the gas phase using resonantly enhanced multiphoton ionization (REMPI) and laser-induced fluorescence (LIF) spectroscopy. Results from two different REMPI experiments provided strong evidence that, after photoexcitation to the S_1 state, bare molecules were funneled into and trapped in a dark state via fast internal conversion. Lifetimes of this dark state were determined to be tens to hundreds of nanoseconds, depending on the internal energy and the degree of methyl substitution. The mass spectra of hydrated thymine clusters demonstrated dependence on the excitation wavelength, and the gradual loss of the ion signal with increasing water content across the absorption region of the S_1 state indicated a reduced lifetime of the S_1 state by the water solvent. In addition, the lifetime of the dark state also decreased gradually as thymine became more hydrated. On the basis of these results, we conclude that, in water solutions, the decay from the S_1 state should be essentially fast internal conversion to the ground state, in agreement with studies from the liquid phase. Our work reveals that the photostability is not an intrinsic property of these pyrimidine bases. Rather, it is the water solvent that stabilizes the photophysical and photochemical behavior of these bases under UV irradiation.

Introduction

The photophysical and photochemical properties of electronically excited states of nucleic acids are crucial to the understanding of the mechanism of DNA photodamage. During the past 4 decades, efforts have been made in the study of the relaxation dynamics of excited nucleic acid bases. In the condensed phase, the lifetimes of the first electric dipole allowed excited state (S_1) of the nucleic acid bases are generally short, on the order of 1 ps.[1−9] This ultrashort lifetime has been suggested to be the reason for the adoption of these bases as the building blocks of the genetic code during the early stages of life's evolution.[8] The mechanism of the fast decay process has been proposed to be internal conversion (IC) to the ground state.[5,8,10] In the gas phase, however, we observed a dark state in the decay of several methyl-substituted pyrimidine bases. We then proposed that, instead of internal conversion to the ground state, the majority of the pyrimidine bases were actually trapped in this dark state for several tens of nanoseconds.[11] Most of the studies in the condensed phase were conducted in water solutions. It is therefore unclear whether the conclusions from the condensed phase referred to the intrinsic properties of these molecules or were a result of their interaction with the water solvent. In this report, we present gas-phase observations of the decay pathways of several methyl-substituted pyrimidine bases and their water complexes. This work will bridge the observations in the two different phases and reveal the role of the solvent in modifying the photophysics of these bases.

Studies on isolated nucleic acid bases in the gas phase have been limited mainly due to the nonvolatility of these compounds. Nevertheless, work on the purine bases reported obvious discrepancies with those from the condensed phase. Using laser desorption, Nir et al. probed the first excited state of guanine.[12] The authors showed evidence that internal conversion was not the dominant decay channel at low temperatures and in the absence of solvent interactions. Piuzzi et al. carried out more detailed studies using IR−UV hole burning.[13] For all of the four tautomers of guanine in the gas phase, the decay lifetimes were observed to be in the nanosecond range. Instead of direct internal conversion to the ground state, decay to a nearby $^1n\pi^*$ state via strong vibronic mixing was therefore tentatively proposed. This photophysical model involving two interacting electronic states was also evoked by Kim and co-workers and de Vries and co-workers in their own studies of adenine.[14,15] With use of picosecond time-resolved 1+1′ photoionization, the lifetime of the first electronically excited state of adenine was determined by Lührs et al.[16] The authors also cast doubt on the generally believed model that involved direct IC to the ground state after photoexcitation. The possibility of either to a low-lying $n\pi^*$ state through IC or to a triplet state via intersystem crossing (ISC) was suggested.

The existence of a dark state in the decay pathway of the nucleic acid bases has been proposed in several theoretical studies.[17,18] Broo suggested that, in adenine, a strong mixing between the lowest $n\pi^*$ and $\pi\pi^*$ states via the out-of-plane vibrational modes could lead to increased overlap with the vibrational states of the ground state.[17] This "proximity effect", as suggested by Lim,[19] was used in the past to explain the ultrashort lifetimes of the DNA bases. A more recent work by Sobolewski et al. proposed that it was the lowest $\sigma\pi^*$ state that was responsible for the fast internal conversion of nitrogen-heterocyclic compounds.[18] However, to the best of the authors' knowledge, there is no available calculation on the lifetime of the dark state and the related quantum yield.

In contrast to the purine bases, experimental studies on the pyrimidine bases are even more limited. However, indications of different decay pathways from that of the condensed phase also exist. The possibility of a low-lying state that couples with

* To whom correspondence should be addressed. Phone: 541-737-6714. Fax: 541-737-2062. E-mail: kongw@chem.orst.edu.

10.1021/jp036553o CCC: $27.50
Published on Web 01/16/2004

the S_1 state was suggested by Levy and co-workers to explain the broad featureless spectra of uracil and thymine in jet-cooled gas-phase experiments.[20] The work on cytosine by De Vries' group reported a long-lived dark state with a lifetime of nearly 300 ns.[21] The authors attributed this state to a triplet state only accessible in the gas phase. Recently, Kang et al. measured the lifetimes of all five nucleic acid bases using the pump−probe technique in the femtosecond regime.[22] In addition to a fast component with a decay time of 6.4 ps, a relatively long-lived state (longer than 100 ps) was observed in thymine, indicating the existence of an alternative pathway. On the basis of energetic analysis, they also attributed this channel to a triplet state. Our previous study on methyl-substituted uracil and thymine confirmed the existence of such a long-lived dark state.[11] However, just on the basis of the energetics and the scale of the lifetime, we were unsure of the multiplicity of the dark state. In fact, we suspected a singlet $n\pi^*$ state instead of a triplet state.

Several attempts have been made to decipher the effect of hydration on the photophysics of nucleic acid bases. Experimental efforts include mass spectroscopy and ionization potential measurements of gas-phase hydration complexes of thymine and adenine,[23] fragmentation pattern analysis of hydrated adenine and thymine,[24,25] UV spectroscopy of hydrated guanine formed in a supersonic jet,[13] and femtosecond pump−probe ionization mass spectroscopy of hydrated adenine clusters.[26] Theoretical studies on the interaction between these bases with water molecules have also been performed.[27−29] Despite these efforts, however, the effect of hydration on the relaxation dynamics of electronically excited states remains unclear. This understanding is crucial not only in terms of revealing the true origin of the photostability of nucleic acid bases, but also in reconciling the differences between results from the gas phase and those from the condensed phase. In this article, we report investigations of hydrated clusters of thymine using resonantly enhanced multiphoton ionization (REMPI). Similar to bare molecules, hydrated clusters also decay via a dark state, although the lifetime of this dark state decreases gradually as thymine becomes more hydrated. An interesting observation is that, in the REMPI experiment, there was almost no signal from hydrated clusters when the excitation laser scanned across the entire absorption region of the S_1 state. We suspect that, in these complexes, the interaction between thymine and water greatly enhances the corresponding conical intersections and, consequently, the lifetime of the S_1 state becomes too short to sustain a detectable population using our nanosecond laser system.

Experimental Details

The experimental apparatus was a standard molecular beam machine with a time-of-flight mass spectrometer (TOF-MS) and a pulsed valve for supersonic cooling. The sample was housed and heated in the nozzle to obtain sufficient vapor pressure, and the operational temperature was 130 °C for 1,3-dimethyluracil (DMU), 150 °C for 1-methyluracil (MU), 180 °C for 1,3-dimethylthymine (DMT), and 220 °C for thymine. No indication of thermal decomposition was observed at these temperatures. The vapor was seeded in 2 atm of helium gas, and the gaseous mixture was expanded into a vacuum chamber at a 10 Hz repetition rate through a 1-mm orifice. Water complexes were formed by bubbling the carrier gas through a room-temperature water reservoir (vapor pressure: ~23 mbar) before being routed to the heated sample. The sample 1-MD, 1,3-DMU, and thymine were purchased from Aldrich Co. and used without further purification. 1,3-DMT was synthesized from thymine,[30] and its purity was checked by nuclear magnetic resonance (NMR) and infrared absorption (IR) spectra.

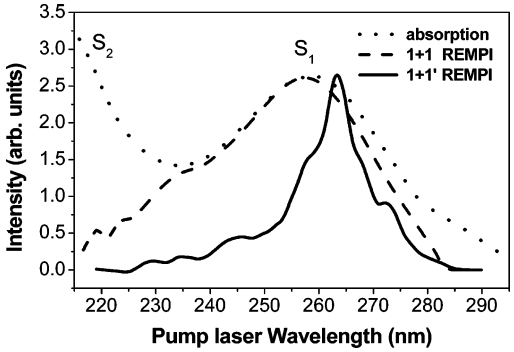

Figure 1. 1+1 REMPI, 1+1′ REMPI, and UV absorption spectra of 1,3-DMU. The 1+1′ REMPI spectrum was obtained by scanning the pump laser and setting the probe laser at 220 nm with a delay time of 10 ns. Neither REMPI spectrum was normalized by the laser power, and at the blue edge of the figure, the low output power of the OPO laser resulted in the missing S_2 feature in the 1+1 spectrum. The absorption spectrum was taken at 140 °C, the same temperature of the pulsed valve during the REMPI experiments.

A Nd:YAG (Continuum, Powerlite 7010) pumped OPO laser (Continuum, Panther) and a Nd:YAG (Spectra Physics GCR 230) pumped dye laser (LAS, LDL 2051) were used in these experiments. In the REMPI experiment, the two lasers were set to counterpropagate; and the light path, the flight tube, and the molecular beam were mutually perpendicular. The delay time between the two lasers was controlled by a delay generator (Stanford Research, DG535). Two different types of 1+1′ REMPI experiments were performed, by scanning either the resonant or the ionization laser. In the laser-induced fluorescence (LIF) experiment, the molecular beam was intercepted by the laser beam from the OPO laser; and the signal was detected by a photomultiplier tube (PMT, Thorn EMI 9125B) through two collection lenses in the direction opposite the molecular beam. To reject the scattered light, masks were used to cover all the windows and lenses, and cutoff filters were inserted in front of the PMT. Using a Tektronix TDX350 digital oscilloscope, the time resolution of the fluorescence signal was essentially limited by the width of the laser pulse (~5 ns). The wavelength region of the fluorescence signal was determined using long pass filters.

Results

Bare Compounds. Figure 1 shows the 1+1 (one color) REMPI and 1+1′ (two color) REMPI spectra together with the gas-phase UV absorption spectrum of 1,3-DMU. In the one-color experiment, a second-order dependence of the ion signal on the laser intensity was observed, while in the two-color experiment, the single-photon nature of each excitation step was confirmed from a linear dependence of the ion signal on both laser beams. The delay between the pump and the probe laser was 10 ns, and the probe laser was set at 220 nm in the 1+1′ experiment. The two features in the UV absorption spectrum were assigned as the first and second excited singlet state, S_1 and S_2, and both were believed to have $\pi\pi^*$ characters.[31] The one-color REMPI spectrum more or less traces the absorption curve for the S_1 feature, while the missing S_2 feature is solely a result of the low output power of the OPO laser. Limited by the nonflat tuning curve of the OPO laser, artificial structures caused by the scanning laser were observed and smoothed out. For this very reason, neither REMPI spectrum was normalized by the intensity of the OPO laser. When divided by the square of the laser power, the one-color REMPI spectrum indeed peaked up again in the vicinity of the S_2 feature. The absorption spectrum was taken at 140 °C, while the REMPI spectra were obtained from a supersonic jet with the pulsed valve heated to

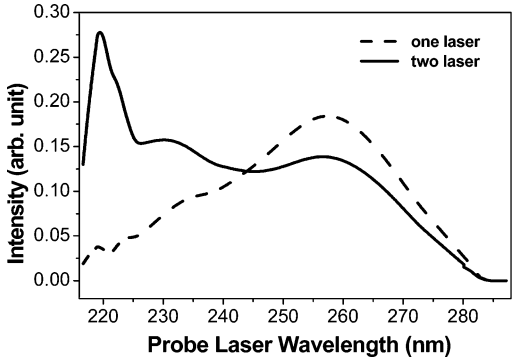

Figure 2. Effect of the pump laser at 250 nm with a time advance of 10 ns on the one-laser REMPI of the probe laser. Both spectra were recorded using the same intensity for the probe laser. The pump laser in the two-laser experiment resulted in a maximum depletion of 20−25% in the region between 245 and 280 nm and an enhancement of 3 decades at 220 nm. See text for a detailed explanation of the experimental method and the implications of this result.

the same temperature. Supersonic cooling might be the reason for the slightly higher energy onset of the 1+1 spectrum. The 1+1′ REMPI spectrum, on the other hand, shows clear discrepancies compared with the one-color spectrum. It has a much narrower feature between 285 and 240 nm, and its center for the S_1 feature is slightly shifted to a lower energy. Under the same experimental conditions, no two-color signal was obtained when the resonant laser scanned further into the S_2 region, even after taking into account the low output power of the OPO laser. Since the only difference between the two REMPI experiments is the delayed ionization (10 ns) by another laser beam at 220 nm, this result is a manifestation of the dynamical behaviors of the excited states.

Figure 2 shows the result of a different REMPI experiment: the first pump laser was set at 250 nm, while the delayed (10 ns) ionization laser scanned through the UV region. The spectra are composites of seven segments, each spanning an adjacent wavelength region of 5 nm. For each segment, we first scanned the OPO laser to obtain the one-color REMPI spectrum (dashed curve), and the two-photon nature of this measurement was confirmed from a power-dependent study. Then with the dye laser beam set at 250 nm and fired 10 ns before the arrival of the OPO laser, we scanned the same wavelength region again using the same OPO laser with **the same power** to obtain the two-laser spectrum (solid curve). The power of the dye laser was carefully controlled so that it generated no ion signal. It is worth noting that this two-laser experiment is not a typical 1+1′ REMPI experiment, and it is referred to as a "two-laser" experiment in the following. When the OPO scanned through the region between 240 and 217 nm, a first-order dependence of the two-laser ion signal on the power of the dye laser was obtained. Quite opposite to the one-color spectrum, the two-laser spectrum shows a sharp rise at the blue edge despite the drop in the power of the OPO laser. Qualitatively, a 30-fold increase in the ion signal at 220 nm was observed. In contrast, when the OPO laser was at a wavelength between 245 and 280 nm, the early arrival of the pump laser caused a depletion of ∼25% of the one-color ion signal. Deviation of the pump wavelength from 250 nm did not result in any difference in the degree of depletion so long as the pump wavelength was within the absorption profile of the S_1 state. Similar to Figure 1, neither spectrum was normalized by the power of the OPO laser, and the precise shapes of the observed features are unimportant to the present discussion. The major issue is that if the S_1 state were short-lived and could decay to the ground state through

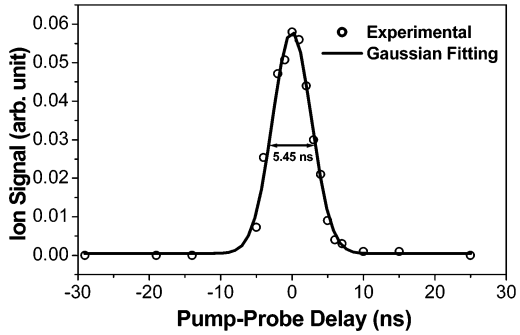

Figure 3. Pump−probe transient ionization signal of 1,3-DMU in the gas phase with the pump and probe wavelengths at 265 and 248 nm, respectively. The time constant (full-width at half-maximum) for the Gaussian function is 5.45 ns.

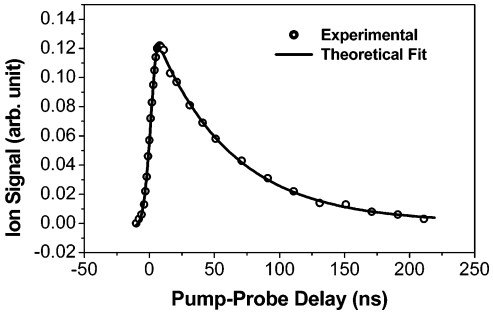

Figure 4. Pump−probe transient ionization signal of 1,3-DMU in the gas phase with the pump and probe wavelengths at 251 and 220 nm, respectively. Hollow circles represent experimental data and the solid line is a theoretical fit including a single-exponential decay convoluted with the instrumental response obtained from Figure 3. The exponential decay constant is 56 ns.

fast IC, 10 ns after excitation, a full recovery of the ground-state population would be expected, and the pump laser should have no effect on the two laser signal. The depletion effect in Figure 2 manifests the existence of a population trap in the decay pathway of the S_1 state, while the enhancement further indicates that the trap can be illuminated under a higher excitation energy.

In the two types of REMPI experiment of Figure 1 and Figure 2, dependence of the signal strength on the delay time between the pump and the probe lasers has been observed. Figure 3 shows a pump−probe transient of 1,3-DMU with both laser beams in the S_1 region: the pump beam at 265 nm, with the probe beam at 248 nm. The profile is fitted by a Gaussian function with a time constant (full-width at half-maximum) of 5.54 ns. Kang et al. reported the lifetimes of the S_1 state of the pyrimidine bases to be in the range of several picoseconds using their femtosecond laser system.[22] Thus, we believe that the time constant of 5.54 ns reflects the response time of our instrument.

Figure 4 shows the pump−probe transient of 1,3-DMU with the pump wavelength at 251 nm and the probe wavelength at 220 nm. On the scale of the figure, the ion signal due to either one laser alone was insignificant, and the overall signal intensity showed linear dependence on the power of each laser. The signal reached its maximum at a delay time of 8 ns between the two beams, and then it decayed to the background level exponentially. Obviously, the decay process in this figure is different from that in Figure 3, and the involvement of another totally different state, that is, a dark state, is implied. Under this assumption, we would expect that the observed time evolution should contain two components: one exponential component corresponding to the decay of the population from the dark state and the other Gaussian component corresponding to the decay of the S_1 state together with the instrumental response. However,

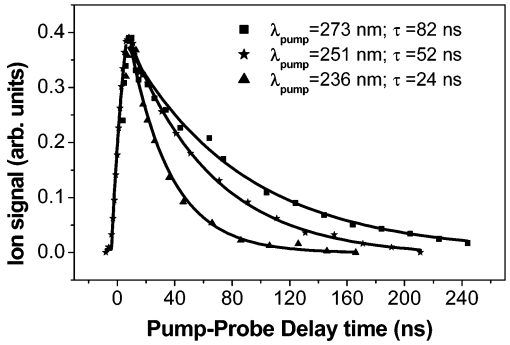

Figure 5. Pump−probe transients of 1,3-DMU in the gas phase at different excitation wavelengths.

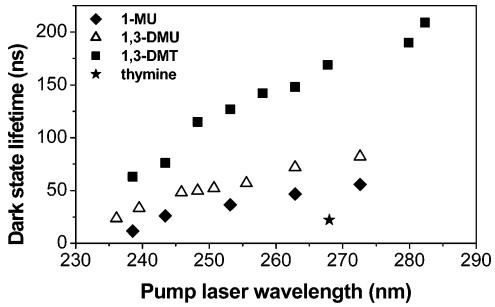

Figure 6. Lifetimes of 1-methyl uracil, 1,3-dimethyl uracil, 1,3-dimethyl thymine, and thymine at different excitation wavelengths.

decomposition of the decay profile indicated that the weight of the Gaussian component was negligible compared with that of the exponential component. In other words, the decay curve showed a single-exponential property.

The lifetime of this dark state demonstrates explicit dependence on the wavelength of the pump beam. With the probe laser fixed at 220 nm, the lifetime of the dark state at different pump wavelengths ranging from 236 to 273 nm is shown in Figure 5. All decay curves have been normalized to have the same amplitude, and the solid lines represent the best fits to the recorded data. The lifetime of the dark state increases gradually as the pump wavelength is increased. For 1,3-DMU, this value ranges from 23 ns at 236 nm to 82 ns at 273 nm. It is worth noting that although the lasers propagate normal to the jet expansion axis, drifting of the molecular beam within a delay time of 300 ns between the two lasers is still negligible. The decay constants in Figure 5 are therefore not contaminated by this instrumental effect.

The number and position of substituted methyl groups on the uracil ring also affect the lifetime of this dark state. Figure 6 summarizes the results on the four pyrimidine bases investigated in this work. The general trend is that the more substituted the ring and the longer the pump wavelength, the longer the lifetime of the dark state. Moreover, substitution at the −1 position is more effective than that at the −5 position in stabilizing the dark state of the monosubstituted bases.

To further assess the fate of the molecules in the excited state, we attempted to observe the fluorescence signal, but the signal was so weak that a quantitative measurement of the spectrum was impossible with our existing setup. However, by recording the decay profile, the fluorescence lifetimes were obtained at different pump wavelengths. Figure 7 shows two typical fluorescence decay curves. The oscillations in these profiles were caused by an electrical problem of our detection system. All decays could be fitted to single-exponential functions, with constants ranging from 18 ns at 236 nm to 54 ns at 260 nm for 1,3-DMU. These values were obtained without corrections of

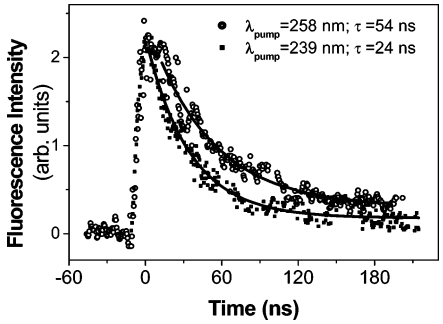

Figure 7. Fluorescence signal of 1,3-DMU in the gas phase at different excitation wavelengths. Solid curves are best fits to the experimental data. The oscillations in the decay curves were caused by an electrical problem in our detection system.

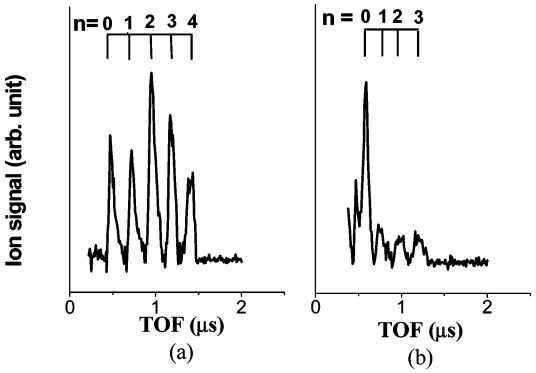

Figure 8. One-color REMPI mass spectra of hydrated thymine clusters, obtained at the excitation wavelengths of 229 nm (a) and 268 nm (b), respectively.

the instrumental response, so they should be regarded as qualitative rather than quantitative. Nevertheless, these fluorescence lifetimes are in good agreement with the decay time of the REMPI signals of Figure 6. Using long pass filters, we determined that the peak of the radiation was centered between 370 and 440 nm.

Hydrated Clusters. To investigate the hydration effect on the properties of the excited states of these bases, we attempted similar experiments on solvated water clusters. However, because a few H-bonding sites were occupied by methyl groups in 1-MU, 1,3-DMU, and 1,3-DMT, we were only successful in generating sufficient thymine−water complexes $T(H_2O)_n$ in our molecular beam. During this experiment, the heating condition and helium stagnation pressure were carefully adjusted to minimize the formation of thymine dimer. At a typical laser intensity of 1 MW/cm^2 (OPO laser), the one-color two-photon mass spectrum demonstrated dependence on the excitation wavelength as shown in Figure 8. These spectra were obtained at the excitation wavelengths of 229 nm (a) and 268 nm (b), respectively. From 220 to 240 nm (the absorption region of the S_2 state of the bare molecule), small water clusters with n up to 4 were readily observable, while in the region of 240−290 nm (the absorption region of the S_1 state of the bare molecule), these hydrated cluster ions were conspicuously missing or barely detectable.

The ratios of ion intensities between hydrated clusters $T(H_2O)_n$ and bare thymine as a function of the excitation wavelength are displayed in Figure 9. These ratios are normalized at 220 nm (S_2 state) to highlight the dynamics at the S_1 state. At 220 nm, all cluster ions with $n \leq 5$ can be clearly seen, suggesting the existence of the corresponding neutral clusters in our source. In the absorption region of the S_1 state, however, the attachment of one water molecule decreases the

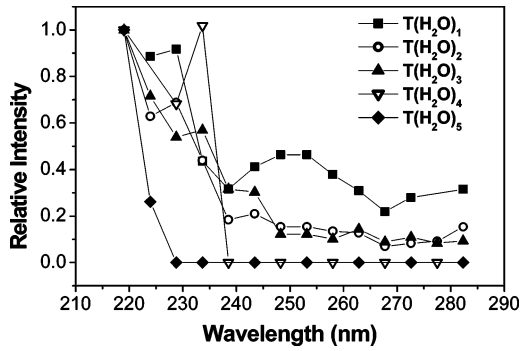

Figure 9. Ratios of ion intensities between the hydrated clusters $T(H_2O)_n$ and bare thymine as a function of the excitation wavelength. The ratios were normalized at 220 nm (S_2 state) to highlight the dynamics at the S_1 state.

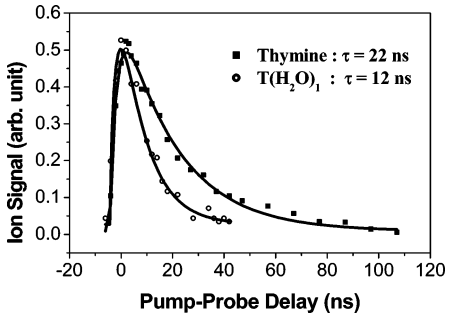

Figure 10. Pump−probe transients of bare thymine and $T(H_2O)_1$ in the gas phase with the pump and probe wavelengths at 267 and 220 nm, respectively.

ion signal to half of its value compared with that of the bare molecule. Additional attachment of one or two water molecules has a similar effect. When four or more water molecules are attached, the S_1 state is no longer observable from the ionization spectra. Since the ionization potential (IP) of thymine is 9.15 eV, corresponding to 271 nm in this one-laser experiment, and $T(H_2O)_n$ clusters are believed to have even lower IPs,[23] the lack of heavy ions in the S_1 region cannot be attributed to the insufficiency of the excitation photon energy. This dramatic loss of heavy ions in the S_1 region should therefore be a result of a loss during excitation or ionization. It is worth noting that although fragmentation has been known to be a recalcitrant problem in studies of clusters, fortunately in this case, it has no effect on our conclusion.

Figure 10 compares the transients of thymine and $T(H_2O)_1$ obtained from a two-color 1+1′ experiment. With the pump wavelength set at 267 nm and the ionization wavelength at 220 nm, the lifetimes of the dark state of thymine and $T(H_2O)_1$ were measured to be 22 and 12 ns, respectively. The fact that the decay profile of $T(H_2O)_1$ contains only a single exponential decay function is evidence that this measurement was not contaminated by dissociative products of larger complexes. For clusters with two or three water molecules attached, the two-color signals were too weak for determination of the decay constants. However, as we increased the delay time between the pump and the probe laser, we observed that heavier clusters disappeared faster than lighter ones. We therefore conclude that this decrease in lifetime with increasing water content is gradual in complexes with $n < 5$. No two-color ion signals were observable for clusters with four or more water molecules.

Discussion

Decay Mechanism of the Pyrimidine Bases. Our results provide concrete evidence that the decay mechanism of methyl-substituted uracil and thymine bases relies heavily on the environment. Figure 11 shows the proposed energy levels and processes for the pyrimidine bases in the gas phase. After initial excitation to the S_1 state, we believe that a significant fraction of the gas-phase molecules decay to a dark state S_d. While the lifetime of the S_1 state is shorter than our instrumental response, the lifetime of the dark state is in the range of tens to hundreds of nanoseconds, depending on the degree of methylation and the amount of excess energy. The nature of this dark state is most likely a low-lying $^1n\pi^*$ state, and further ionization from this dark state requires a much higher excitation energy. Although we are unable to provide a precise estimate of the quantum yield for this decay channel, based on our previous estimate, the lower limit should be 20% in bare molecules.[11] Water molecules, on the other hand, can significantly reduce the lifetime of the S_1 state and enhance the IC from the dark state to the ground state. As a result, in aqueous solutions, the dark state becomes essentially undetectable. The S_2 state, on the other hand, follows an entirely different pathway, as indicated by the lack of two laser signals for the bare compound in Figure 1 and the existence of all four water complexes in Figure 8. It is worth noting that this model should be applicable to all pyrimidine bases given their similar behaviors in the gas phase and in the liquid phase, despite the fact that we were only successful in studies of thymine−water complexes.

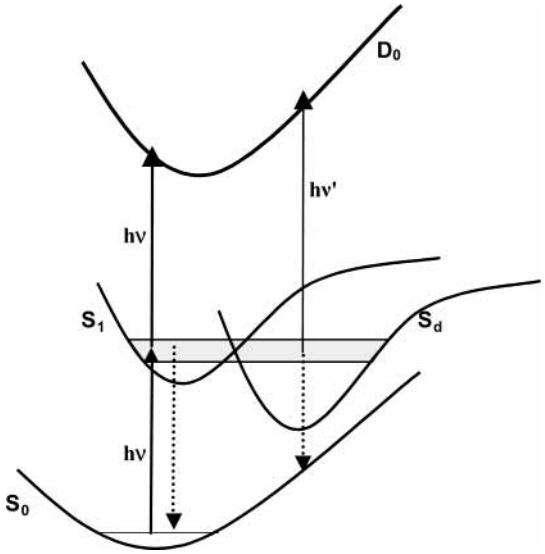

Figure 11. Proposed potential energy surfaces and processes for the pyrimidine bases. Ionization from the S_1 state and the dark state S_d samples a different Franck−Condon region of the ionic state, resulting in different ionization energies for these two states.

This model can provide a consistent explanation of our experimental observations. The 1+1′ REMPI signal in Figure 1 (solid line) is from ionization of this dark state, while the one-color signal is from ionization of the molecules initially populated in the S_1 state. The narrower width of the 1+1′ spectrum compared with that of the one-color spectrum reflects the limited energy range for effective overlap between the dark state and the S_1 state. This dark state does not absorb in the region of 245−280 nm; rather, it absorbs in a much higher energy region from 217 to 245 nm. Relaxation of the molecular frame in the dark state could result in a different Franck−Condon region for vertical ionization, thereby increasing the ionization energy for the dark state. In the REMPI experiment of Figure 2, this shift in absorption profile of the excited species causes the depletion of the two-laser signal when the probe wavelength is between 245 and 280 nm. When the probe laser

scans into the absorption region of this dark state, an enhanced ion yield is observable. The decay process in Figure 4 corresponds to the decay of this dark state. Fluorescence from this dark state should take place in a red-shifted region, that is, 370−440 nm from this study, compared with that of the S_1 state (300 nm).[32] The similarity of the decay constants of the fluorescence (Figure 7) and the 1+1′ REMPI signal (Figures 4 and 5) confirms that, in both experiments, we are probing the same dark state. Methyl substitution stabilizes this dark state as shown in Figure 6, while more vibrational energy obtained from the initial excitation step destabilizes this state by opening more decay channels (Figures 5 and 6). The loss of ion signal in the S_1 region of Figure 9 with the addition of water molecules is caused by the decreased lifetime of the S_1 state. This decrease is a result of enhanced vibronic coupling between the S_1 state and the dark state or the ground state, due to the presence of H_2O molecules.

The existence of the dark state and the above decay mechanism are also supported by previous experimental and theoretical results. The work on cytosine in the gas phase by De Vries' group also reported a long-lived dark state with a lifetime of nearly 300 ns.[21] On the basis of the scale of the lifetime, however, the authors suggested the involvement of a triplet state. Kang et al. reported two decay components for thymine in the gas phase using the femtosecond pump−probe ionization technique.[22] The slower component with an estimated lifetime of more than 100 ps corresponded to a state within the same energy region as our dark state, though the authors also suspected the involvement of a triplet state based on energetic analysis. Brady et al. observed the broad and diffusive feature of the S_1 state in their gas phase study of uracil and thymine.[20] The authors attributed the featureless spectrum to either mixing of electronic states or a large geometry change between the ground and excited electronic states. A recent theoretical investigation on cytosine showed the existence of a state switch between $\pi\pi^*$ and $n_O\pi^*$ (the lone pair electron on the oxygen atom) states.[33] The crossing between the two states was weakly avoided and there existed a small energy barrier between the equilibrium position of the $^1n_O\pi^*$ state and its intersection with the ground state. This barrier might be the very reason that the majority of the molecules are trapped in the dark state after the $^1\pi\pi^*-^1n\pi^*$ internal conversion. More detailed calculations of the decay process from the $^1n_O\pi^*$ state to the ground state will be revealing, as suggested by the authors.

Effect of Hydration on the Photophysics of the Excited State. The reduction or complete loss of the one-color ion signal for hydrated clusters near the absorption region of the S_1 state (Figure 9) signifies a reduction of lifetime for these clusters. Under our experimental conditions using a nanosecond laser system, the failure to accumulate a population at the S_1 state for further ionization can only be attributed to fast depopulation from the initially prepared state, through internal conversion, intersystem crossing, or dissociation. Kim and co-workers studied hydrated adenine clusters in the gas phase.[24,26] Using a nanosecond laser, they observed a near complete loss of hydrated adenine ions in the S_1 region, while with use of a femtosecond laser, all hydrated clusters were observable. They also measured the lifetime of the S_1 state to be 230 fs for $A(H_2O)_1$ and 210 fs for $A(H_2O)_2$, while the lifetime of the S_1 state of bare adenine was 1 ps. This 5-fold change in lifetime was apparently sufficient to cause qualitatively different behavior under femtosecond or nanosecond excitation.

Lifetime reduction upon hydration should be no surprise based on studies in the gas phase and the liquid phase. For thymine, the lifetime of the S_1 state was reported to be 6.4 ps in the gas phase[22] and 1.2 ps in the liquid phase.[6] Similarly, for the other two pyrimidine bases, uracil and cytosine, the lifetimes of the S_1 states were measured to be 2.4 and 3.2 ps respectively in the gas phase,[22] while these values decreased to 0.9 and 1.1 ps in the liquid phase.[6] The measurement related to Figure 9 further confirms that this lifetime reduction is a gradual process with increasing water content. When four or more water molecules are in the vicinity, we suspect that the behavior of thymine is essentially the same as that in the liquid phase, i.e., the lifetime of the S1 state should be on the picosecond time scale. Further experiments in the femtosecond regime is under preparation.

The reason for the lifetime reduction of the S_1 state should be faster internal conversion upon hydration. In the work of Wanna et al. on pyrazine and pyrimidine, a similar loss of ion signal from hydrated clusters was observed,[34] and an increased rate of internal conversion upon solvation was proposed. In the case of the pyrimidine bases, however, we could not distinguish the destination of the increased IC being either the dark state or the ground state, although indications from our experimental data, including the faster decay of the dark state upon hydration in Figure 10, favor the dark state as the destination. Typically in a $n\pi^*$ transition, solvation by a proton donor such as water causes a blue shift, while in a $\pi\pi^*$ transition, this effect is a slight red shift.[35] The energy gap between the initially accessed $\pi\pi^*$ (S_1) and the $n\pi^*$ dark state can thus be reduced in the presence of water, and subsequently a better vibronic coupling between the two states can occur. On the other hand, we cannot exclude the possibility that IC directly to the ground state might still be somewhat competitive with IC to the dark state even in the gas phase. In the presence of water, the balance between the two decay pathways could shift, and a faster direct IC process to the ground state could also reduce the lifetime of the S_1 state.

The weak two-color ion signal and the reduced lifetime of the dark state in Figure 10 further indicate a faster decay process of the dark state for hydrated clusters. Limited by the signal-to-noise ratio in our experiment, we could not extract the lifetimes of larger clusters. However, as we increased the delay time between the pump and the probe laser, we observed that heavier clusters disappeared faster than lighter ones. We therefore conclude that, with increasing water content, the lifetime of the dark state should also demonstrate a gradual decrease. In the liquid phase, it is likely that the dark state is so short-lived that it is beyond detection using typical femtosecond pump−probe techniques. We propose that the reason for this lifetime reduction is a decrease in the barrier for the conical intersection between the dark state and the ground state. In the gas phase,[11] this conical intersection is thought to be responsible for the low fluorescence quantum yield of the $^1n\pi^*$ dark state, and the barrier effectively blocks this intersection from easy access. However, solute−solvent interactions can shift the relative positions of the involved states and therefore lower the barrier for the intersection.

This observation on the effect of hydration can reconcile the differences between results from the gas phase and those from the liquid phase. In the liquid phase, the dark state is no longer as stable as that in the gas phase, and a fast cascade from the S_1 state via the dark state to the ground state becomes essentially indistinguishable from a direct IC process to the ground state. Alternatively, one could also interpret the lifetime reduction of the S_1 state as an indication of increased yield of the IC process directly to the ground state due to the presence of water. In either explanation, the photophysics of the pyrimidine bases is

significantly affected by the water solvent. The origin of the photostability of the pyrimidine bases therefore lies in the environment, not in the intrinsic property of these bases.

In Figure 9, the total loss of cluster ions in the S_1 region for $T(H_2O)_n$ when $n \geq 4$ and the failure to observe any two-color signal for these ions suggest the completion of the first solvation shell with four water molecules. This result is consistent with a previous study by Kim et al.[25] On the basis of the fragmentation pattern of hydrated thymine clusters, the authors deduced a well-defined hydration shell structure, and the first hydration shell was composed of only four water molecules. It is this first solvation shell that dramatically changes the photophysical property of thymine. In this sense, four water molecules are sufficient to capture the essence in modeling these pyrimidine bases in a solution environment.

Our conclusion on the hydration of thymine molecules is different from that of adenine. In the study of $A(H_2O)_n$, a complete loss of cluster ions, including those with $n < 4$, was observed for all sized clusters in the S_1 region. The authors attributed this loss to the dissociative $^1n\pi^*$ state upon hydration.[24] The basis of this statement was that according to their preliminary calculation and a theoretical result,[36] solvent water molecules preferred to form a water cluster before solvating the adenine molecule. The severance of one water−adenine bond was therefore sufficient to eliminate all the solvent molecules. For the pyrimidine bases, however, theoretical studies showed that water molecules bind to the pyrimidine ring at three different primary sites in a shell-like structure.[37,38] In Figure 9, the signal loss for $T(H_2O)_n$ displayed a clear *n*-dependence; and the total loss of cluster ions only occurred when $n \geq 4$. This result is clearly different from that of $A(H_2O)_n$.

Conclusions

We present here evidence for a decay mechanism of uracil and thymine bases in the gas phase and the strong effect of solvation by water molecules. After photoexcitation to the S_1 state, a bare molecule is funneled into and trapped in a dark state with a lifetime of tens to hundreds of nanoseconds. The nature of this dark state is most likely a low-lying $^1n\pi^*$ state. Solvent molecules affect the decay pathways by increasing IC from the S_1 to the dark state or to the ground state and from the dark state to the S_0 state. The lifetimes of the S_1 state and the dark state are decreased with the addition of only one or two water molecules. When more than four water molecules are attached, the photophysics of these hydrated clusters should rapidly approach that in the condensed phase. We are currently in preparation of a femtosecond experiment to further elucidate the energetics and lifetimes of the dark state.

Our gas-phase results reveal an important function of water in protecting our genetic code from photodamage. The high ionization yield of bare base molecules from the dark state by deep UV radiation, as shown in Figure 2, indicates that the photostability of our genetic code is not an intrinsic property of the bases themselves. Rather, the interaction of these bases with water molecules provides the necessary relaxation mechanism for the excited species. Quenching by solvent molecules may be the key for the photostability of the pyrimidine bases in DNA and RNA.

Our work on hydrated clusters manifests the value of gas-phase experiments. Condensed phase studies reveal the properties of the bulk system. However, it is difficult to distinguish intrinsic vs collective properties of a system. Gas-phase studies, on the other hand, directly provide information on bare molecules. Moreover, the investigation of size-selected water complexes can mimic the transition from an isolated molecule to the bulk. The comparison of gas-phase experimental results with theoretical calculations can also provide a direct test of theoretical models.

Acknowledgment. This work was supported by the National Science Foundation, the Petroleum Research Foundation, and the Alfred P. Sloan Foundation. The skillful synthesis of 1,3-DMT by T. Suyama is deeply appreciated.

References and Notes

(1) Daniels, M.; Hauswirth, W. *Science* **1971**, *171*, 675−677.
(2) Callis, P. R. *Annu. Rev. Phys. Chem.* **1983**, *34*, 329−357.
(3) Nikogosyan, D. N.; Angelov, D.; Soep, B.; Lindqvist, L. *Chem. Phys. Lett.* **1996**, *252*, 322−326.
(4) Häupl, T.; Windolph, C.; Jochum, T.; Brede, O.; Hermann, R. *Chem. Phys. Lett.* **1997**, *280*, 520−524.
(5) Reuther, A.; Nikogosyan, D. N.; Laenen, R.; Laubereau, A. *J. Phys. Chem.* **1996**, *100*, 5570−5577.
(6) Reuther, A.; Iglev, H.; Laenen, R.; Laubereau, A. *Chem. Phys. Lett.* **2000**, *325*, 360−368.
(7) Pecourt, J.-M. L.; Peon, J.; Kohler, B. *J. Am. Chem. Soc.* **2000**, *122*, 9348−9349.
(8) Pecourt, J.-M. L.; Peon, J.; Kohler, B. *J. Am. Chem. Soc.* **2001**, *123*, 10370−10378.
(9) Gustavsson, T.; Sharonov, A.; Markovitsi, D. *Chem. Phys. Lett.* **2002**, *351*, 195−200.
(10) Andréasson, J.; Holmén, A.; Albinsson, B. *J. Phys. Chem. B* **1999**, *103*, 9782−9789.
(11) He, Y.; Wu, C.; Kong, W. *J. Phys. Chem. A* **2003**, *107*, 5145−5148.
(12) Nir, E.; Grace, L.; Brauer, B.; de Vries, M. S. *J. Am. Chem. Soc.* **1999**, *121*, 4896−4897.
(13) Piuzzi, F.; Mons, M.; Dimicoli, I.; Tardivel, B.; Zhao, Q. *Chem. Phys.* **2001**, *270*, 205−214.
(14) Kim, N. J.; Jeong, G.; Kim, Y. S.; Sung, J.; Kim, S. K. *J. Chem. Phys.* **2000**, *113*, 10051−10055.
(15) Nir, E.; Kleinermanns, K.; Grace, L.; de Vries, M. S. *J. Phys. Chem. A* **2001**, *105*, 5106−5110.
(16) Lührs, D. C.; Viallon, J.; Fischer, I. *Phys. Chem. Chem. Phys.* **2001**, *3*, 1827−1831.
(17) Broo, A. *J. Phys. Chem. A* **1998**, *102*, 526−531.
(18) Sobolewski, A. L.; Domcke, W.; Dedonder-Lardeux, C.; Jouvet, C. *Phys. Chem. Chem. Phys.* **2002**, *4*, 1093−1100.
(19) Lim, E. C. *J. Phys. Chem.* **1986**, *90*, 6770−6777.
(20) Brady, B. B.; Peteanu, L. A.; Levy, D. H. *Chem. Phys. Lett.* **1988**, *147*, 538−543.
(21) Nir, E.; Müller, M.; Grace, L. I.; de Vries, M. S. *Chem. Phys. Lett.* **2002**, *355*, 59−64.
(22) Kang, H.; Lee, K. T.; Jung, B.; Ko, Y. J.; Kim, S. K. *J. Am. Chem. Soc.* **2002**, *124*, 12958−12959.
(23) Kim, S. K.; Lee, W.; Herschbach, D. R. *J. Phys. Chem.* **1996**, *100*, 7933−7937.
(24) Kim, N. J.; Kang, H.; Jeong, G.; Kim, Y. S.; Lee, K. T.; Kim, S. K. *J. Phys. Chem. A* **2000**, *104*, 6552−6557.
(25) Kim, N. J.; Kim, Y. S.; Jeong, G.; Ahn, T. K.; Kim, S. K. *Int. J. Mass Spectrom.* **2002**, *219*, 11−12.
(26) Kang, H.; Lee, K. T.; Kim, S. K. *Chem. Phys. Lett.* **2002**, *359*, 213−219.
(27) Del Bene, J. E. *J. Comput. Chem.* 1981, *2*, 200−206.
(28) Marian, C. M.; Schneider, F.; Kleinschmidt, M.; Tatchen, J. *Eur. Phys. J. D* **2002**, *20*, 357−367.
(29) Sobolewski, A. L.; Domcke, W.; Dedonder-Lardeux, C.; Jouvet, C. *Phys. Chem. Chem. Phys.* **2002**, *4*, 1093−1100.
(30) Hedayatullah, M. J. *Heterocycl. Chem.* **1981**, *18*, 339−342.
(31) Clark, L. B.; Peschel, G. G.; Tinoco, I., Jr. *J. Phys. Chem.* **1965**, *69*, 3615−3618.
(32) Becker, R. S.; Kogan, G. *Photochem. Photobiol.* **1980**, *31*, 5−13.
(33) Ismail, N.; Blancafort, L.; Olivucci, M.; Kohler, B.; Robb, M. A. *J. Am. Chem. Soc.* **2002**, *124*, 6818−6819.
(34) Wanna, J.; Menapace, J. A.; Bernstein, E. R. *J. Chem. Phys.* **1986**, *85*, 1795−1805.
(35) Brealey, G. J.; Kasha, M. *J. Am. Chem. Soc.* **1955**, *77*, 4462−4468.
(36) Périquet, V.; Moreau, A.; Carles, S.; Schermann, J. P.; Desfrançois, C. *J. Electron. Spectrosc.* **2000**, *106*, 141−151.
(37) Gaigeot, M.-P.; Ghomi, M. *J. Phys. Chem. B* **2001**, *105*, 5007−5017.
(38) Marian, C. M.; Schneider, F.; Kleinschmidt, M.; Tatchen, J. *Eur. Phys. J. D* **2002**, *20*, 357−367.